Environmental Science & Technology

Article

Cite This: Environ. Sci. Technol. 2018, 52, 2819−2826

pubs.acs.org/est

Impacts of the Degradation of 2,3,3,3-Tetrafluoropropene into Trifluoroacetic Acid from Its Application in Automobile Air Conditioners in China, the United States, and Europe

Ziyuan Wang,[†,‡] Yuhang Wang,[*,‡] Jianfeng Li,[‡] Stephan Henne,[§] Boya Zhang,[†] Jianxin Hu,[†] and Jianbo Zhang[*,†]

[†]State Key Joint Laboratory for Environmental Simulation and Pollution Control, College of Environmental Sciences and Engineering, Peking University, Beijing 100871, China

[‡]School of Earth and Atmospheric Sciences, Georgia Institute of Technology, Atlanta, Georgia 30332, United States

[§]Laboratory for Air Pollution/Environmental Technology, Empa, Swiss Federal Laboratories for Materials Science and Technology, Uberlandstrasse 129, Dübendorf 8600, Switzerland

Supporting Information

ABSTRACT: HFO-1234yf (2,3,3,3-tetrafluoropropene) was proposed as an automobile air conditioner (MAC) refrigerant worldwide. However, its atmospheric degradation product is the highly soluble and phytotoxic trifluoroacetic acid (TFA), which persists in aquatic environments. We used a global three-dimensional chemical transport model to assess the potential environmental effects resulting from complete future conversion of the refrigerant in all MAC to HFO-1234yf in China, the United States, and Europe. The annual mean atmospheric concentrations of HFO-1234yf were 2.62, 2.20, and 2.73 pptv, and the mean deposition rates of TFA were 0.96, 0.45, and 0.52 kg km^{-2} yr^{-1}, in three regions. The regional TFA deposition sources mainly came from emissions within the same region. The annual TFA deposition in the North Pole region was lower than the global average and mainly originated from European emissions. A potential doubling in the future HFO-1234yf emissions in China mainly affected the local TFA depositions. The TFA concentrations in rainwater were strongly affected by the regional precipitation rates. North Africa and the Middle East, regions with scant rainfall, had extremely high TFA concentrations. The rainwater concentrations of TFA during individual rain events can exceed the level considered to be safe, indicating substantial potential regional risks from future HFO-1234yf use.

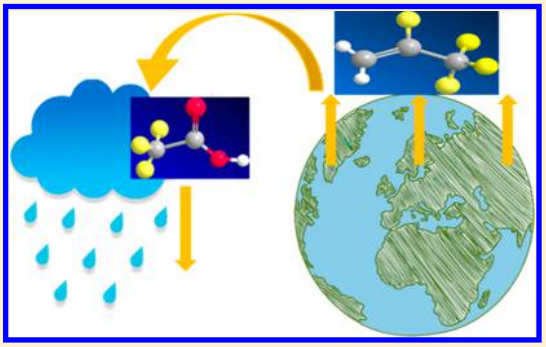

INTRODUCTION

Hydrofluorocarbons (HFCs), which have zero ozone depletion potentials (ODPs), were introduced and widely used as alternatives to older ozone depletion substances (ODSs) such as chlorofluorocarbons (CFCs) and hydrochlorofluorocarbons (HCFCs).[1,2] However, most HFCs are potent greenhouse gases (GHGs) with high global warming potentials (GWPs) and contribute to radiative forcing.[3,4] The worldwide use and atmospheric concentrations of HFCs have increased dramatically in the past decade, and its future CO_2-equivalent emissions are projected to continue growing and impact the global climate.[5,6] In October 2016, as an amendment to the Montreal Protocol, a global agreement was reached to limit the future use of HFCs (Kigali amendment). Most developed countries should begin to reduce HFCs use by 2019, and two groups of developing countries should freeze their use by 2024 and 2028, respectively.

Under this agreement, HFC-134a (1,1,1,2-tetrafluoroethane), which is used as a cooling agent in more than 80% of passenger and commercial vehicles worldwide, is now facing an upcoming phase-out.[6] With a GWP of 4, a promising replacement hydrofluoro-olefin, HFO-1234yf (2,3,3,3-tetrafluoropropene), was proposed[7] and is already commercially applied in the European Union (F-gas regulation) and the United States. After being released, HFO-1234yf mostly reacts with OH radicals and chlorine radicals to yield trifluoroacetyl fluoride (TFF), although some reacts with O_3 and NO_3.[8,9] In the presence of water, TFF hydrolyzes rapidly into trifluoroacetic acid (TFA), which is finally removed from the atmosphere by dry and wet deposition. HFO-1234yf has an olefinic bond, which has a higher atmospheric reactivity, a shorter atmospheric lifetime of ∼12 days, and an ∼100% yield of TFF.[8−10] In contrast, the currently used HFCs that produce TFA, such as HFC-134a, have a longer atmospheric lifetime of ∼14.6 years and a smaller TFF yield of 7−20%.[11,12] These facts suggest that TFA deposition will be enhanced and more

Received: November 21, 2017
Revised: January 16, 2018
Accepted: January 30, 2018
Published: January 30, 2018

DOI: 10.1021/acs.est.7b05960
Environ. Sci. Technol. 2018, 52, 2819−2826

localized if HFO-1234yf is used instead of HFC-134a with the same emission rates.

TFA is a mildly phytotoxic strong organic acid and is persistent and highly soluble in water, with a lifetime of thousands of years.[13−16] Constant concentrations of TFA in deep oceans have indicated that natural sources of TFA exist in the oceans.[17−19] Research indicates that an anthropogenic source, especially the atmospheric oxidation of HFCs, contributes to the majority of the TFA in the atmosphere, in precipitation, and in surface waters.[20] Current levels of TFA from HFCs oxidation are not thought to threaten the most sensitive aquatic life.[11,14,20,21]

However, the potentially higher deposition rates from widespread use of newer alternatives such as HFO-1234yf suggest that a re-examination would be beneficial. Similar studies were conducted in the United States (US) and Europe (EU),[22−24] but no such study was performed in China (CH), which is likely to be a major future source of automobile air conditioning (MAC) use. Additionally, these former studies did not consider the regional interactions at a larger scale or the seasonal variations of HFO-1234yf annual emissions due to their temporal and spatial constraints. In this study, we use a global-scale atmospheric chemistry transport model to examine the potential environmental impact of a complete transition to HFO-1234yf as the cooling agent in MACs in CH, the US, and EU. This is the first time that emissions from different regions have been simulated in large-scale models and that interregional effects have been assessed. We made a one-year simulation to predict the amount of atmospheric HFO-1234yf and its conversion to TFA, local deposition, regional transport, and interactions.

METHODS

Emissions. The refrigerant emission inventory of HFO-1234yf in China was developed based on our former inventory using a bottom-up method that considered direct and indirect emissions from the manufacturing, operation, servicing, and end-of-life disposal of MACs.[25] Because of the currently booming and predicted future expansion of China's automobile industry, we considered two emissions scenarios: (1) a current scenario using the current number of vehicles in the year 2016 and (2) a future scenario that used projected vehicle numbers for the year 2030. Both scenarios assumed that all vehicles were equipped with HFO-1234yf as a refrigerant and used adapted high-leak factors. State-level emissions were allocated to county-level data based on the GDP and population weighting and further regriding to 1° × 1° grids based on roadway distributions and on-road activity data.

Luecken et al.[23] assumed that all vehicles in the US would be equipped with HFO-1234yf in 2017 and calculated the US refrigerant emission inventory for low and high scenarios. They allocated state-level emissions into county-level ones and to 36 km grids covering the continental US. Henne et al.[22] estimated that HFO-1234yf emissions from European (i.e., 27 European Union countries plus Croatia, Norway, Switzerland, and Turkey) MACs in 2020 using low and high scenarios with lower and upper limits for emission factors projected vehicle numbers and the assumption of a complete replacement of HFC-134a by HFO-1234yf. Country total emissions were allocated according to population density and on-road CO emissions. We adopted their high scenarios emission inventories, both distributed to 1° × 1° grids and applied in this study as inputs.

Seasonal allocations of annual emissions were made assuming that all the operation leakage, irregular leakage, and servicing leakage occur during the summer and are equally distributed into June, July, and August.[26] End-of-life leakages were allocated across all 12 months equally. Emissions from different regions were tagged as HFO-1234yf-CH, HFO-1234yf-US, and HFO-1234yf-EU in models to track their transport and impacts. Regional and inter-regional impacts were researched by setting different emission inputs: (1) input all three emission regions; (2) input CH emissions and zero out the US and EU emissions; and (3) repeat step 2 for the US and EU emissions.

In this study, only emissions from the world's three largest automobile ownership regions were included, and both the regional and inter-regional environmental effects from these regions were considered.

GEOS-Chem Model Description. We used the global three-dimensional chemical transport model (CTM) GEOS-Chem version v11-02. GEOS-Chem is driven by GEOS-FP assimilated meteorological data from the NASA Goddard Earth Observing System (GEOS). We used 2° × 2.5° horizontal grid resolution and 72 vertical layers for simulation. The wet scavenging scheme for aerosols is described by Liu et al.[27] and Wang et al.[28], and the scheme for gases is by Amos et al.[29] Dry deposition was calculated using a standard resistance-in-series model applied to a surface-type database from Olson.[30−32] Nonrefrigerant emissions were extracted from the EDGAR-v42 for global base emissions and superseded by regional inventories for the US (EPA NEI 2011), Europe (EMEP),[33] Canada (CAC),[34] Mexico (BRAVO),[35] and Asia.[36] NO_x-O_x-hydrocarbon-aerosol simulations were adapted as the chemistry mechanism, including oxidant (OH, O_3, NO_x, and Cl) concentrations.[37] The GEOS-Chem simulation was conducted for the whole year of 2016 following 2 months of spin-up.

Chemical Degradation of HFO-1234yf and Its Products. We represented the chemical degradation of HFO-1234yf and the production of TFA by extending the NO_x-O_x-hydrocarbon-aerosol simulation to include the following reactions: HFO-1234yf reacting with (1) OH radicals as the dominant degradation pathway with a temperature-dependent rate constant of 1.26×10^{-12} $\exp(-35/T)$ cm^3 $molecule^{-1}$ s^{-1} and an ~100% yield of TFF, (2) Cl radicals with a rate constant of 7.03×10^{-11} cm^3 $molecule^{-1}$ s^{-1} and a 92% yield of TFF, (3) O_3 with a rate constant of 2.77×10^{-21} cm^3 $molecule^{-1}$ s^{-1} and a 50% yield of TFF, and (4) NO_3 radicals with a rate constant of 3.0×10^{-15} cm^3 $molecule^{-1}$ s^{-1} and a 91% yield of TFF.[8,9,38] GEOS-Chem simulated OH, O_3, Cl, and NO_3 were used in this study. As previous studies indicated, HFO-1234yf is mostly degraded via OH oxidation and slightly degraded via reactions with Cl, NO_3, and O_3, which is also found in our work based on their reaction rates and concentrations. The intermediate product TFF is unreactive in the gas phase but hydrolyzes to TFA in water.

We added a hydrolysis process to the heterogeneous chemistry of GEOS-Chem and applied a Henry's Law solubility constant of 3 M atm^{-1} at a standard temperature of 298.15 K and a hydrolysis rate of 150 s^{-1} of the dissolved TFF.[39,40] We assumed that the partitioning of TFF between the gaseous and aqueous phases is at a pseudosteady state, and we calculated the dissolved quantities of TFF in grid boxes using its Henry's Law constant and the total volume of cloudwater presented in the grids. No research concerning pH effects on the hydrolysis of TFF or the dehydration of TFA were reported, so these effects were not included.

DOI: 10.1021/acs.est.7b05960
Environ. Sci. Technol. 2018, 52, 2819−2826

Table 1. Summary of Model Results for HFO-1234yf and TFA

	CH annual[a]	US annual[a]	US summer[a]	US summer[b] by Luecken et al[23]	EU annual[a]	EU annual by Henne et al.[22] FLEXPART[d]	EU annual by Henne et al.[22] STOCHEM[d]	NP annual	globe annual[c]	OT annual
HFO emissions (Gg)	42.65	24.53	15.21	15.21	19.16	19.16	19.16			
mean HFO (pptv)	2.62	2.20	4.19	7.40	2.73	2.60	1.50	0.40	0.34	0.10
max HFO (pptv)	30.96	19.44	40.95	300.00	19.08	18.00	3.70	1.19	30.96	
mean TFA (pptv)	0.48	0.33	0.83	na	0.42	0.10	0.12	0.04	0.07	0.03
max TFA (pptv)	3.77	1.15	3.26	>0.8	1.78	0.60	0.35	0.14	3.77	
mean TFA deposition (kg km^{-2} yr^{-1})	0.96	0.45	0.59	0.48	0.52	0.65	0.76	0.08	0.12	0.05
max TFA deposition (kg km^{-2} yr^{-1})	7.94	2.12	2.90	2.34	2.95	2.50	1.90	0.56	7.94	
mean rainwater conc of TFA (ng L^{-1})	638	480	1277	500[b]	620	580	800	144		
max rainwater conc of TFA (ng L^{-1})	22 574	4485	15 417	1264[b]	2099	1700	2160	549		

[a]Our results under scenario I are given, and the mean and maximum are various spatial aggregates (CH, the US, EU, the NP, and the globe) from the annual and seasonal (summer) means. [b]Luecken et al. simulated the US results for high emission scenario are presented. TFA deposition values during the summertime were scaled-up with the assumption that, during this period, ~50% of the annual HFO-1234yf emissions were released. [c]The global rainwater concentration of TFA was not presented because extreme values affected the comparability of the data. [d]Henne et al. simulated EU annual results for high emission scenario by FLEXPART and STOCHEM models are both presented.

In the gas phase, TFA reacts with OH radicals with a rate constant of 9.35 × 10^{-14} cm^3 molecule^{-1} s^{-1}.[10] TFA is highly soluble in cloudwater and partitions into the gas phase when the cloudwater evaporates. Previous studies did not provide quantitative information for the dependence of the TFA partition on pH, and therefore, the pH effects were not considered. Aqueous TFA is removed by both wet scavenging deposition and dry deposition, using the Henry's Law solubility constant of 9.0 × 10^3 M atm^{-1} at the standard temperature, 298.15 K.[40] Chhantyal-Pun et al. recently found TFA reacts with Criegee intermediates, which are another gas-phase sink of TFA.[41] This process was not included in our study because the atmospheric concentrations of Criegee intermediates are still highly uncertain and they are not simulated explicitly in the model.[42−45]

RESULTS AND DISCUSSION

Atmospheric Mixing Ratios. The model results are presented at different levels of temporal and spatial aggregations. The results of HFO-1234yf emissions from three sources under scenario I were shown in Table 1. Scenario II was calculated for China's future scenario with emissions of 88.4 Gg yr^{-1} and with the same that the US and EU emissions used in scenario I.

The global OH concentration in GEOS-Chem is higher, and the HFO-1234yf lifetime calculated based on the OH field is shorter, compared with former studies. Nielson et al.[18] reported a HFO-1234yf lifetime of ~11 days using an estimated global OH concentration of 1 × 10^6 molecules cm^{-3}. With a Northern Hemisphere mean OH concentration of 1.1 × 10^6 molecules cm^{-3} from GEOS-Chem modeling, the HFO-1234yf lifetime is ~9.35 days. The regional mean HFO-1234yf lifetimes with respect to OH are 5.31 (2.15−25.99) days for CH, 6.13 (2.90−31.97) days for the US, and 7.30 (3.71−33.88) days for EU.

Figure 1 shows the spatial distributions of the annual mean mixing ratios of HFO-1234yf and TFA for scenario I. Figure S1 details the values of HFO-1234yf globally as 0.34 pptv and regionally as 2.62 pptv for CH, 2.20 pptv for the US, 2.73 pptv for EU, 0.40 pptv for the NP, and 0.10 pptv for OT (all other global regions excluding CH, US, and EU). It also shows the annual TFA mixing ratios globally to be 0.07 pptv and

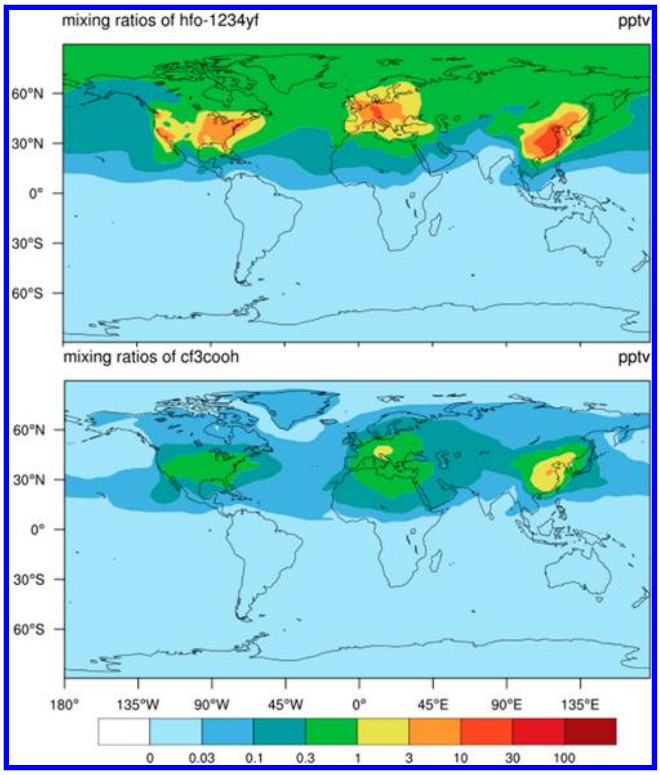

Figure 1. Global annual mean surface mixing ratios (pptv) of HFO-1234yf (upper) and TFA (bottom) under scenario I.

regionally to be 0.48 pptv for CH, 0.33 pptv for the US, 0.43 pptv for EU, 0.04 pptv for the NP, and 0.03 pptv for OT. Despite China's emissions being twice as large as those of the US and EU, all three regional HFO-1234yf and TFA atmospheric concentrations were very close. These differences can partly be explained by (1) the area of CH (2.26 × 10^7 km^2) being larger than those of the US (1.45 × 10^7 km^2) and EU (9.76 × 10^6 km^2) and (2) more TFA deposition in CH (23 392 tons) than in the US (7505 tons) and EU (5869 tons).

The largest simulated annual mean HFO-1234yf concentrations were 30.96 pptv for CH in the eastern and southern coastal areas, 19.44 pptv for the US in the eastern US and

DOI: 10.1021/acs.est.7b05960
Environ. Sci. Technol. 2018, 52, 2819−2826

California, 19.08 pptv for EU in central and western Europe including northern Italy, the Ruhr area, and Paris, and 1.19 pptv for the NP in the regions closest to the three emission regions. The largest annual mean atmospheric concentrations of TFA were 3.77 pptv for CH, 1.15 pptv for the US, and 1.78 pptv for EU. All these peak concentrations occurred in regions with high HFO-1234yf emissions.

There were considerable variations in the seasonal mean HFO-1234yf and TFA concentrations throughout the year, as shown in Figures S1−S3. For the three emission regions, their values peaked in the summer and reached a minimum in the spring. Our summertime mean and maximum HFO-1234yf concentrations were 8.56 and 109 pptv for CH, 4.19 and 40.9 pptv for the US, and 4.96 and 36.4 pptv for EU, respectively, of which the US and EU values were comparable with the previous results.[22,23] Luecken et al.[23] simulated the summertime mean and maximum HFO-1234yf concentrations as 7.4 and 300 pptv. Henne et al.[22] calculated the summertime mean and maximum mixing ratios as 1.5 and 15 pptv, which can be adjusted to 3.6 and 36 pptv after multiplying by a factor of 2.4 on the basis that, in their model, only 25% of the annual emissions occurred during the summer, which was instead assumed to be ∼60% in our study. These differences were mostly due to the different model grid designs for the simulation, especially for that of Luecken et al.,[23] who simulated the US using CMAQ with a 36 km horizontal grid, which would tend to promote higher, localized concentrations. Differences in the chemical mechanism that was used could also affect the OH levels and consequently the lifetime of HFO-1234yf in the atmosphere if the concentrations of oxidants or photolytic fluxes were different. Our results also showed that, in spring, autumn, and winter, the seasonal atmospheric concentrations agreed closely for HFO-1234yf (0.47−0.85 pptv in CH, 1.24−1.91 pptv in the US, and 1.58−2.54 pptv in EU) and for TFA (0.09−0.18 pptv in CH, 0.11−0.23 pptv in the US, and 0.11−0.27 pptv in EU). However, different meteorological conditions in the three seasons would impact the atmospheric chemistry and deposition, causing differences in the seasonal concentrations.

Figure S4 details the global annual mean mixing ratios of HFO-1234yf as 0.51 pptv and TFA as 0.10 pptv under scenario II, and Figure S5 shows their global distributions. With the doubled (with a factor of 2.08) emissions in CH, the atmospheric concentrations in CH approximately doubled, from 2.62 to 5.58 pptv for HFO-1234yf and from 0.48 to 0.95 pptv for TFA. The mixing ratios in the US, EU, and the NP increased only slightly. Changes in the emissions of an area can affect the local atmospheric concentrations directly and considerably but have little effects on the atmospheric components of other regions.

TFA Deposition. Figure 2 shows the predicted dry, wet, and total deposition of TFA under scenario I in 2016. The annual global total TFA deposition from HFO-1234yf emissions from three main sources was 59.71 Gg yr^{-1} (69% of the total emissions, which should be an upper limit considering that the sinks such as reactions with Criegee intermediates were not included in this study). The remainder of the TFA was mainly remaining emissions either accumulated in the atmosphere in the gaseous and aqueous phases during the simulation period or lost through TFA degradation by OH. Dry deposition comprises 5−30% of the total deposition loss, depending on spatial and temporal variations. The maximum deposition occurred during the summer (of both dry and wet depositions),

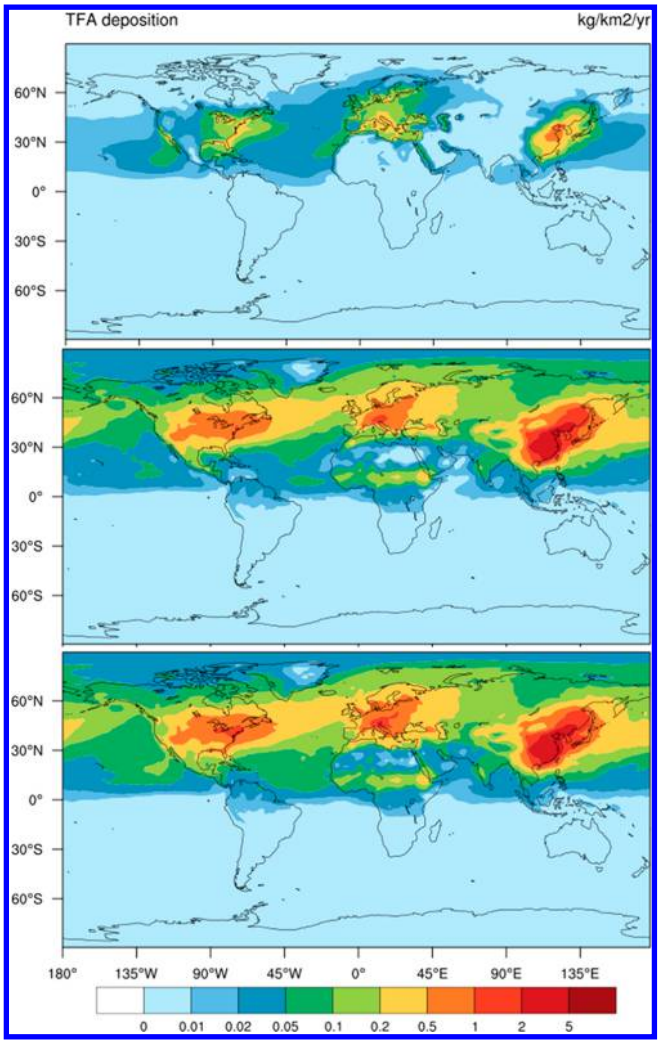

Figure 2. Predicted annual total deposition rates of TFA (kg km^{-2} yr^{-1}) under scenario I from dry deposition (top), wet deposition (middle), and both processes (bottom).

which accounted for 71% of the global yearly depositions, followed by autumn (12%). The TFA deposition depends on the HFO-1234yf emissions as the primary factor, as well as meteorological conditions such convective mass flux and the amount of precipitation.

The annual total depositions of TFA over the three emission regions were 23.39 Gg yr^{-1} in CH, 7.50 Gg yr^{-1} in the US, and 5.87 Gg yr^{-1} in EU, accounting for 55%, 31%, and 31% of their local emissions, respectively. The remainder of the deposition occurred outside the emission areas and was more widely dispersed. The ratio of domestic deposition to emissions reached a minimum during the winter (40% for CH, 17% for the US, and 13% for EU) because the meteorological conditions in winter accelerated atmospheric transport and had less precipitation. This ratio peaked during autumn (149% for CH, 35% for the US, and 31% for EU) because the HFO-1234yf and TFA that had accumulated in the atmosphere during the high, summertime emissions continued to deposit in September. In summer, the deposition to emission ratio in the US increased to 35%, while Kazil et al. only reported a ratio of 17% due to venting from the upper troposphere outside of the region.[24] In addition, differences in the model transport,

DOI: 10.1021/acs.est.7b05960
Environ. Sci. Technol. 2018, 52, 2819−2826

meteorology conditions, cloud treatment, and other factors would all play a role in this different conclusion.

The global annual total deposition rate of TFA was estimated to be 0.12 kg km^{-2} yr^{-1}, while the regional rates had averages of 0.96, 0.45, and 0.52 kg km^{-2} yr^{-1} and maxima of 7.94, 2.12, and 2.95 kg km^{-2} yr^{-1} for CH, the US, and EU, respectively. Our results for the annual deposition of TFA in EU agreed well with those by Henne et al.[22] (means of 0.65 and 0.76 kg km^{-2} yr^{-1} and maxima of 2.5 and 1.9 kg km^{-2} yr^{-1} considering their results from two models). The annual dry deposition rates were largest in the northern China Plain, Bohai Bay, the east coast of the US, and southern EU. In contrast, the largest wet deposition rates appeared in the southeast coastal region of CH, the northeast and middle of the US, and western and central EU. As wet deposition dominated the total TFA deposition, the total deposition distribution pattern was similar to that of wet depositions. The mean summertime total deposition rates of TFA were 0.83 kg km^{-2} for CH, 0.29 kg km^{-2} for the US, and 0.35 kg km^{-2} for EU, as shown in Figure S6, which is very close to the Luecken et al.[23] calculated 0.24 kg km^{-2} summertime deposition for the US.

Under scenario II, with the doubled emissions of HFO-1234yf from China, the annual total depositions of TFA from HFO-1234yf in CH increased linearly to 45.34 Gg yr^{-1} (with a factor of 1.94) and increased slightly in the US and EU to 8.27 and 6.14 Gg yr^{-1} (with factor of 1.10 and 1.05), respectively. Figure S7 shows that deposition rates increased with a similar pattern, to 1.85, 0.50, 0.54, and 0.18 kg km^{-2} yr^{-1} for CH, the US, EU, and the whole globe, respectively. During the summer, the TFA deposition rate in CH reached a mean of 1.52 kg km^{-2} and a maximum of 12.89 kg km^{-2}. The global OH field is not affected by variation in HFO-1234yf emissions, which was also indicated by Luecken et al.[23] and Henne et al.[22] Changes in the emission rates can affect the domestic deposition amounts directly with a nearly linear relationship and can also impact remote areas. Thus, future increases in China's HFO-1234yf emissions may increase both the local amounts of TFA deposition and ecological risks.

Inter-regional Transport and Effects. Figure 3 shows the seasonal and annual mean contributions of the three emission regions to the amounts of HFO-1234yf and TFA in different regions (CH, the US, EU, the NP, and the globe) under scenario I. The atmospheric amounts of HFO-1234yf and TFA and the amount of TFA depositions of the three emissions regions mostly came from emissions within the region, which accounted for 75−95% of the total values. The local emission contributions were smallest during the winter and largest in the summer. This is because (1) the chemical lifetime of HFO-1234yf is shorter and wet deposition by rain is more efficient in summer than winter; (2) transport of the emission region is faster in winter than summer because of higher wind speed. The meteorological conditions in winter accelerate the transport of substances, and those in summer restrain it, which causes more inter-regional transmission and exchange in the winter; and (3) local emissions increased dramatically during the summer compared with the other three seasons, making local emissions the primary factor affecting the regional atmospheric processes.

The largest source of emissions in the NP was EU, contributing to 63% of the HFO-1234yf mixing ratios, 51% of the TFA mixing ratios, and 51% of the TFA depositions (in terms of the annual means). EU contributions were relatively stable across the four seasons, ranging from 59−69% for the

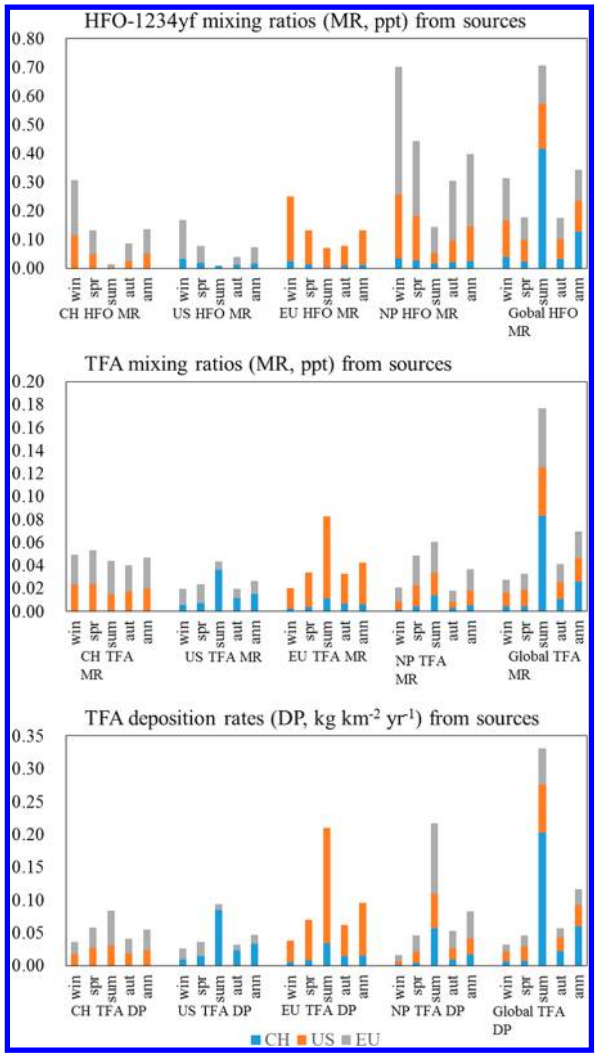

Figure 3. Contributions of emissions from three sources (CH, the US, and EU) to different regional scales (CH, the US, EU, the NP, and the globe), with the seasonal and annual mean values of HFO-1234yf mixing ratios (upper), TFA mixing ratios (middle), and TFA deposition rates (bottom) under scenario I. The seasonal deposition rates were scaled-up to the annual flux.

HFO-1234yf mixing ratios, 45−61% for the TFA mixing ratios, and 50−59% for the TFA depositions. This is not only because northern EU is geographically closest to the NP but also because meteorological conditions facilitate the dispersion of EU emissions northward to the NP. In contrast, CH and the US had much smaller effects on the NP, with CH contributing 6%, 15%, and 21% of the NP's annual HFO-1234yf mixing ratios, TFA mixing ratios, and TFA depositions, respectively, and the US contributing 31%, 34%, and 28%, respectively.

For the other regions, the greatest impacts came from CH's emissions, which were the largest of the three sources. CH's emissions mostly affected neighboring areas, especially for East Asia, including Japan, Korea, and the Pacific coast, and had lower impacts on more remote areas, especially for intercontinental transport. Emissions from the US were mainly transported eastwards to the Atlantic Ocean, even reaching EU, and westwards to the Pacific Ocean, with little dispersion to the north (Canada) or the south (Mexico). EU emissions were also mostly transported to the east and west, reaching as far east as

DOI: 10.1021/acs.est.7b05960
Environ. Sci. Technol. 2018, 52, 2819−2826

the Caspian Sea, Russia, and Kazakhstan, and as far west as the Atlantic Ocean and even eastern America.

Under scenario II, with more-than-doubled HFO-1234yf emissions from CH, CH's contributions to the annual mean TFA mixing ratios and depositions of the US increased from 4.5% to 10.8% and from 7.2% to 15.8%, while the effect on those of EU increased from 1.4% to 3.6% and from 3.0% to 7.2%, respectively. Regional amounts of HFO-1234yf and TFA in the US and EU still came primarily from local emissions. Despite the increased amounts of HFO-1234yf and TFA at the NP coming from CH as its emissions increased, the NP's primary source of emissions was still EU. Scenario II is the maximum hypothesized emissions from CH with no changes to those from the US and EU. These small, insignificant changes in the substance compositions of other regions suggest that future CH emissions would cause environmental effects focused on a local scale, rather than globally. Future substitution of HFO-1234yf for HFCs could ease the global problem of climate change but potentially cause regional environmental risks, particularly by increasing local TFA depositions. EU emissions exert the largest effects on regions near the NP

■ ENVIRONMENTAL IMPLICATIONS

TFA has recently attracted worldwide scientific attention. Studies have found no evidence of TFA in ancient aquatic systems such as groundwater, surface water, or ice,[13,15,18] while they have found levels of TFA in recent rainwater, spring water and surface water. In China, concentrations of TFA ranging from 13.7 to 7850 ng L^{-1} were detected in the tap and surface water of cities,[46] averaging 141 ng L^{-1} in the surface waters of the Pearl River Estuary, 210 ng L^{-1} in its open sea, 279 ng L^{-1} in the coastal waters of Honghai Bay,[46] and 1580 ± 558 pg m^{-3} in the atmosphere.[47] In the US, TFA concentrations in surface waters were found with median values of 21 ng L^{-1} in remote regions and 144 ng L^{-1} in the San Francisco Bay Area.[48] In Europe, TFA was detected in rainwater at 110 ng L^{-1} in southern Germany and in spring water at 16−123 ng L^{-1}, and in Switzerland, in surface water at 81 ng L^{-1} for rivers and 119 ng L^{-1} for lakes.[13,15] The presence of natural TFA sources is still not resolved definitely. Studies have shown that HCFCs and HFCs can degrade into TFA and are considered to be the primary anthropogenic sources.[3,4,20] On the other hand, studies have proved that TFA is naturally present in the oceans, but inconsistent background values have been reported.[17,19]

Our study presented the projected potential future TFA levels in rainwater over a global scale from three emission regions, and the concentrations were calculated using the rain events in the GEOS-Chem meteorological data after a period of TFA formation in the atmosphere (see Figure S9). The annual mean rainwater concentrations of TFA were projected to be 638 ng L^{-1} in CH, 480 ng L^{-1} in the US, 620 ng L^{-1} in EU, and 144 ng L^{-1} in the NP. During the summertime, which had the largest TFA depositions, the mean rainwater concentration of these four regions increased to 1451, 1277, 1762, and 313 ng L^{-1}, respectively. The highest monthly concentrations of TFA in three emission regions were 1.81×10^5 ng L^{-1} in the southern plateau of Tibet in CH during November, 22 223 ng L^{-1} around California and Oregon of the US during August, and 9467 ng L^{-1} in the southern Mediterranean in EU during July. These regions all have scant rainfall during certain seasons, so the TFA is highly concentrated.

Although the total amounts of TFA were higher in the source regions, the TFA rainwater concentrations were extremely high over the regions of North Africa and the Middle East (20° to 40° north and −15° to 60° east). For example, the region's monthly mean concentrations in August were 2.22×10^8 ng L^{-1}, approximately 5 orders of magnitude larger than that of CH, the US, and EU. This area was simulated with the world's lowest amount of rainwater, averaging 1.78×10^{-6} kg m^{-2} s^{-1} (a factor of 20 below the global average for rainwater), with a minimum value of 2.42×10^{-18} kg m^{-2} s^{-1}. This is in contrast to CH, the US, and EU, which have minimum amounts of rainwater of 6.97×10^{-7}, 8.05×10^{-8}, and 5.39×10^{-8} kg m^{-2} s^{-1}, respectively. Although the total TFA depositions in North Africa and the Middle East were small, the concentration of TFA in rainwater greatly exceeded the no-effect level for the most sensitive alga, which has been determined as 1.2×10^5 ng L^{-1}, suggesting that TFA could have an impact on sensitive species in the region. As simulated rainwater amounts in these regions have uncertainties, further determinations of the TFA deposition and the TFA concentrations in rainwater need to be conducted to verify the rates predicted by this and other studies[22,23] and to assess the environmental risks brought by the TFA originating from HFO-1234yf.

The estimation of future emissions of new compounds such as HFO-1234yf is highly uncertain, as is the characterization of global oxidant levels, subgrid cloud and rainfall processes, vertical transport, and other physical and chemical aspects that impact the TFA aqueous concentrations and deposition. Along with earlier studies, the current work helps to better define the uncertainty parameters of this important issue. In addition, future use of HFO-1234yf may not be limited to MACs but may include stationary refrigeration units and manufacturing processes, which would increase the impacts noted in this study. The multipollutant, multiphase impact of potential future increases in emissions of HFO-1234yf and other reactive HFOs is an area where additional research and analysis should be done to more accurately assess both local and global health and environmental impacts.

■ ASSOCIATED CONTENT

Supporting Information

The Supporting Information is available free of charge on the ACS Publications website at DOI: 10.1021/acs.est.7b05960.

Additional description of spatial and temporal aggregation; plots of HFO and TFA mixing ratios; and model outputs of HFO and TFA distributions are provided (PDF)

■ AUTHOR INFORMATION

Corresponding Authors

*Phone: (404) 894-3995; e-mail: yuhang.wang@eas.gatech.edu.

*Phone: +86-10-62753746; e-mail: jbzhang@pku.edu.cn.

ORCID

Jianbo Zhang: 0000-0001-8937-0953

Notes

The authors declare no competing financial interest.

■ ACKNOWLEDGMENTS

We thank Deborah Luecken from the EPA for providing data on the U.S. HFO-1234yf emissions and for insightful help on atmospheric chemistry and modeling. This work was supported

DOI: 10.1021/acs.est.7b05960
Environ. Sci. Technol. 2018, 52, 2819−2826

by the National Natural Science Foundation of China (nos. 41775143 and 41575140).

REFERENCES

(1) World Meteorological Organization. *Scientific Assessment of Ozone Depletion: 2006*; WMO: Geneva, Switzerland, 2007; Vol. *50*, p 572.

(2) United Nations Environment Programme. *Handbook for the Montreal Protocol on Substances that Deplete the Ozone Layer*, 9th ed.; UNEP: Nairobi, Kenya, 2012.

(3) Metz, B.; Solomon, S.; Kuijpers, L.; Andersen, S. O.; Davidson, O.; Pons, J.; de Jager, D.; Kestin, T.; Manning, M.; Meyer, L. *Safeguarding the Ozone Layer and the Global Climate System: Issues Related to Hydrofluorocarbons and Perfluorocarbons*; Cambridge University Press: New York, 2005.

(4) Montzka, S.; Reimann, S.; O'Doherty, S.; Engel, A.; Krüger, K.; Sturges, W. T. Ozone-Depleting Substances (ODSs) and Related Chemicals. In *Scientific Assessment of Ozone Depletion: 2010*; World Meteorological Organization: Geneva, Switzerland, 2011.

(5) Gschrey, B.; Schwarz, W.; Elsner, C.; Engelhardt, R. High increase of global F-gas emissions until 2050. *Greenhouse Gas Meas. Manage.* **2011**, *1* (2), 85−92.

(6) Velders, G. J.; Fahey, D. W.; Daniel, J. S.; McFarland, M.; Andersen, S. O. The large contribution of projected HFC emissions to future climate forcing. *Proc. Natl. Acad. Sci. U. S. A.* **2009**, *106* (27), 10949−10954.

(7) Orkin, V. L.; Martynova, L. E.; Ilichev, A. N. High-Accuracy Measurements of OH Reaction Rate Constants and IR Absorption Spectra: CH2CF−CF3 and trans-CHFCH−CF3. *J. Phys. Chem. A* **2010**, *114* (19), 5967−5979.

(8) Nielsen, O. J.; Javadi, M. S.; Sulbaek Andersen, M. P.; Hurley, M. D.; Wallington, T. J.; Singh, R. Atmospheric chemistry of CF3CFCH2: Kinetics and mechanisms of gas-phase reactions with Cl atoms, OH radicals, and O3. *Chem. Phys. Lett.* **2007**, *439* (1), 18−22.

(9) Papadimitriou, V.; Talukdar, R.; Portmann, R. W.; Ravishankara, A. R.; Burkholder, J. CF3CF═CH2 and (Z)-CF3CF═CHF: temperature dependent OH rate coefficients and global warming potentials. *Phys. Chem. Chem. Phys.* **2008**, *10* (6), 808.

(10) Hurley, M. D.; Wallington, T. J.; Javadi, M. S.; Nielsen, O. J. Atmospheric chemistry of CF3CFCH2: products and mechanisms of Cl atom and OH radical initiated oxidation. *Chem. Phys. Lett.* **2008**, *450* (4), 263−267.

(11) Tang, X.; Madronich, S.; Wallington, T.; Calamari, D. Changes in tropospheric composition and air quality. *J. Photochem. Photobiol., B* **1998**, *46* (1−3), 83−95.

(12) Wallington, T. J.; Hurley, M. D.; Fracheboud, J. M.; Orlando, J. J.; Tyndall, G. S.; Sehested, J.; Møgelberg, T. E.; Nielsen, O. J. Role of excited CF3CFHO radicals in the atmospheric chemistry of HFC-134a. *J. Phys. Chem.* **1996**, *100* (46), 18116−18122.

(13) Berg, M.; Müller, S. R.; Mühlemann, J.; Wiedmer, A.; Schwarzenbach, R. P. Concentrations and mass fluxes of chloroacetic acids and trifluoroacetic acid in rain and natural waters in Switzerland. *Environ. Sci. Technol.* **2000**, *34* (13), 2675−2683.

(14) Boutonnet, J. C.; Bingham, P.; Calamari, D.; Rooij, C. D.; Franklin, J.; Kawano, T.; Libre, J.; McCul-loch, A.; Malinverno, G.; Odom, J. M.; et al. Environmental risk assessment of trifluoroacetic acid. *Hum. Ecol. Risk Assess.* **1999**, *5* (1), 59−124.

(15) Jordan, A.; Frank, H. Trifluoroacetate in the environment. Evidence for sources other than HFC/HCFCs. *Environ. Sci. Technol.* **1999**, *33* (4), 522−527.

(16) Lifongo, L. L.; Bowden, D. J.; Brimblecombe, P. Thermal degradation of haloacetic acids in water. *Int. J. Phys. Sci.* **2010**, *5* (6), 738−747.

(17) Frank, H.; Christoph, E. H.; Holm-Hansen, O.; Bullister, J. L. Trifluoroacetate in ocean waters. *Environ. Sci. Technol.* **2002**, *36* (1), 12−15.

(18) Nielsen, O. J.; Scott, B. F.; Spencer, C.; Wallington, T. J.; Ball, J. C. Trifluoroacetic acid in ancient freshwater. *Atmos. Environ.* **2001**, *35* (16), 2799−2801.

(19) Scott, B. F.; Macdonald, R. W.; Kannan, K.; Fisk, A.; Witter, A.; Yamashita, N.; Durham, L.; Spencer, C.; Muir, D. Trifluoroacetate profiles in the Arctic, Atlantic, and Pacific oceans. *Environ. Sci. Technol.* **2005**, *39* (17), 6555−6560.

(20) Tang, X.; Wilson, S. R.; Solomon, K. R.; Shao, M.; Madronich, S. Changes in air quality and tropospheric composition due to depletion of stratospheric ozone and interactions with climate. *Photoch. Photobio. Sci.* **2011**, *10* (2), 280−291.

(21) Hanson, M. L.; Solomon, K. R. Haloacetic acids in the aquatic environment. Part II: ecological risk assessment. *Environ. Pollut.* **2004**, *130* (3), 385−401.

(22) Henne, S.; Shallcross, D. E.; Reimann, S.; Xiao, P.; Brunner, D.; O'Doherty, S.; Buchmann, B. Future emissions and atmospheric fate of HFC-1234yf from mobile air conditioners in Europe. *Environ. Sci. Technol.* **2012**, *46* (3), 1650−1658.

(23) Luecken, D. J.; Waterland, R. L.; Papasavva, S.; Taddonio, K. N.; Hutzell, W. T.; Rugh, J. P.; Andersen, S. O. Ozone and TFA impacts in North America from degradation of 2, 3, 3, 3-tetrafluoropropene (HFO-1234yf), a potential greenhouse gas replacement. *Environ. Sci. Technol.* **2010**, *44* (1), 343−348.

(24) Kazil, J.; McKeen, S.; Kim, S. W.; Ahmadov, R.; Grell, G. A.; Talukdar, R. K.; Ravishankara, A. R. Deposition and rainwater concentrations of trifluoroacetic acid in the United States from the use of HFO-1234yf. *Journal of Geophysical Research-Atmospheres* **2014**, *119* (24), 14059−14079.

(25) Su, S.; Fang, X.; Li, L.; Wu, J.; Zhang, J.; Xu, W.; Hu, J. HFC-134a emissions from mobile air conditioning in China from 1995 to 2030. *Atmos. Environ.* **2015**, *102*, 122−129.

(26) Papasavva, S.; Hill, W. R.; Andersen, S. O. GREEN-MAC-LCCP: a tool for assessing the life cycle climate performance of MAC systems. *Environ. Sci. Technol.* **2010**, *44* (19), 7666−7672.

(27) Liu, H.; Jacob, D. J.; Bey, I.; Yantosca, R. M. Constraints from 210Pb and 7Be on wet deposition and transport in a global three-dimensional chemical tracer model driven by assimilated meteorological fields. *Journal of Geophysical Research-Atmospheres* **2001**, *106* (D11), 12109−12128.

(28) Wang, Q.; Jacob, D. J.; Fisher, J. A.; Mao, J.; Leibensperger, E. M.; Carouge, C. C.; Le Sager, P.; Kondo, Y.; Jimenez, J. L.; Cubison, M. J.; et al. Sources of carbonaceous aerosols and deposited black carbon in the Arctic in winter-spring: implications for radiative forcing. *Atmos. Chem. Phys.* **2011**, *11* (23), 12453−12473.

(29) Amos, H. M.; Jacob, D. J.; Holmes, C. D.; Fisher, J. A.; Wang, Q.; Yantosca, R. M.; Corbitt, E. S.; Galarneau, E.; Rutter, A. P.; Gustin, M. S.; et al. Gas-particle partitioning of atmospheric Hg (II) and its effect on global mercury deposition. *Atmos. Chem. Phys.* **2012**, *12* (1), 591−603.

(30) NOAA National Geophysical Data Center. Digital raster data on a 10 min geographic 1080 × 2160 grid. In *Global Ecosystems Database*, Version 1.0: Disc A; National Centers for Environmental Information: Boulder, CO, 1992.

(31) Wang, Y.; Jacob, D. J.; Logan, J. A. Global simulation of tropospheric O3-NO x-hydrocarbon chemistry: 1. Model formulation. *Journal of Geophysical Research-Atmospheres* **1998**, *103* (D9), 10713−10725.

(32) Wesely, M. L. Parameterization of surface resistances to gaseous dry deposition in regional-scale numerical models. *Atmos. Environ.* **1989**, *23* (6), 1293−1304.

(33) Vestreng, V.; Klein, H. *Emission Data Reported to UNECE/EMEP: Quality Assurance and Trend Analysis & Presentation of WebDab*; Norwegian Meteorological Institute: Oslo, Norway, 2002.

(34) *National Pollutant Release Inventory*. http://www.ec.gc.ca/pdb/cac/cachomee.cfm.

(35) Kuhns, H.; Knipping, E. M.; Vukovich, J. M. Development of a United States−Mexico emissions inventory for the big bend regional aerosol and visibility observational (BRAVO) study. *J. Air Waste Manage. Assoc.* **2005**, *55* (5), 677−692.

(36) Streets, D. G.; Bond, T. C.; Carmichael, G. R.; Fernandes, S. D.; Fu, Q.; He, D.; Klimont, Z.; Nelson, S. M.; Tsai, N. Y.; Wang, M. Q.;

DOI: 10.1021/acs.est.7b05960
Environ. Sci. Technol. 2018, 52, 2819−2826

et al. An inventory of gaseous and primary aerosol emissions in Asia in the year 2000. *J. Geophys. Res.* **2003**, *108* (D21), 8809.
(37) Henze, D. K.; Hakami, A.; Seinfeld, J. H. Development of the adjoint of GEOS-Chem. *Atmos. Chem. Phys.* **2007**, *7* (9), 2413−2433.
(38) Papadimitriou, V. C.; Lazarou, Y. G.; Talukdar, R. K.; Burkholder, J. B. Atmospheric Chemistry of CF3CFCH2 and (Z)-CF3CFCHF: Cl and NO3 Rate Coefficients, Cl Reaction Product Yields, and Thermochemical Calculations. *J. Phys. Chem. A* **2011**, *115* (2), 167−181.
(39) George, C.; Saison, J. Y.; Ponche, J. L.; Mirabel, P. Kinetics of mass transfer of carbonyl fluoride, trifluoroacetyl fluoride, and trifluoroacetyl chloride at the air/water interface. *J. Phys. Chem.* **1994**, *98* (42), 10857−10862.
(40) Sander, R. Compilation of Henry's law constants (version 4.0) for water as solvent. *Atmos. Chem. Phys.* **2015**, *15* (8), 4399−4981.
(41) Chhantyal-Pun, R.; McGillen, M.; Beames, J.; Khan, A.; Percival, C.; Shallcross, D.; Orr-Ewing, A. Temperature Dependence of the Rates of Reaction of Trifluoracetic Acid with Criegee Intermediates. *Angew. Chem., Int. Ed.* **2017**, *56* (56), 9044−9047.
(42) Novelli, A.; Hens, K.; Tatum Ernest, C.; Martinez, M.; Nölscher, A. C.; Sinha, V.; Paasonen, P.; Petäjä, T.; Sipilä, M.; Elste, T.; et al. Estimating the atmospheric concentration of Criegee intermediates and their possible interference in a FAGE-LIF instrument. *Atmos. Chem. Phys.* **2017**, *17* (12), 7807−7826.
(43) Vereecken, L.; Novelli, A.; Taraborrelli, D. Unimolecular decay strongly limits the atmospheric impact of Criegee intermediates. *Phys. Chem. Chem. Phys.* **2017**, *19* (47), 31599−31612.
(44) McGillen, M. R.; Curchod, B. F.; Chhantyal-Pun, R.; Beames, J. M.; Watson, N.; Khan, M. A. H. H.; McMahon, L.; Shallcross, D. E.; Orr-Ewing, A. J. Criegee Intermediate−Alcohol Reactions, A Potential Source of Functionalized Hydroperoxides in the Atmosphere. *ACS Earth and Space Chemistry* **2017**, *1*, 664.
(45) Newland, M. J.; Rickard, A. R.; Sherwen, T.; Evans, M. J.; Vereecken, L.; Muñoz, A.; Ródenas, M.; Bloss, W. J. The atmospheric impacts of monoterpene ozonolysis on global stabilised Criegee intermediate budgets and SO2 oxidation: experiment, theory and modelling. *Atmos. Chem. Phys. Discuss.* **2017**, 1−65.
(46) Wang, Q.-Y.; Ding, X.; Wang, X.-M. Preliminary study of trifluoroacetic acid in surface waters of the Pearl River Estuary and neighboring eastern offshore sea area. *J. Trop. Oceanogr.* **2010**, *29* (1), 46−50.
(47) Wu, J.; Martin, J. W.; Zhai, Z.; Lu, K.; Li, L.; Fang, X.; Jin, H.; Hu, J.; Zhang, J. Airborne trifluoroacetic acid and its fraction from the degradation of HFC-134a in Beijing, China. *Environ. Sci. Technol.* **2014**, *48* (7), 3675−3681.
(48) Cahill, T. M.; Seiber, J. N. Regional distribution of trifluoroacetate in surface waters downwind of urban areas in Northern California, USA. *Environ. Sci. Technol.* **2000**, *34* (14), 2909−2912.

DOI: 10.1021/acs.est.7b05960
Environ. Sci. Technol. 2018, 52, 2819−2826